Cancellation of reference update-induced 1/f noise in chirped-pulse DAS

PEDRO J. VIDAL-MORENO,[1,*] ETIENNE ROCHAT,[2] PABLO FERMOSO,[1] MARÍA R. FERNÁNDEZ-RUIZ, [1,3] HUGO MARTINS, [3] SONIA MARTIN-LOPEZ, [1] MANUEL OCAÑA, [1] MIGUEL GONZALEZ-HERRAEZ[1]

[1] *Department of Electronics, University of Alcalá, Polytechnic School, 28805, Madrid, Spain*
[2]*Omnisens S.A. Av. de Riond-Bosson 3, 1110 Morge, Switzerland*
[3] *Daza de Valdés Institute of Optics (IO-CSIC), Serrano St., 121, 28006, Madrid, Spain*
**Corresponding author: pedro.vidal@edu.uah.es* mailto:author_three@uni-jena.de

Received XX Month XXXX; revised XX Month, XXXX; accepted XX Month XXXX; posted XX Month XXXX (Doc. ID XXXXX); published XX Month XXXX

Distributed acoustic sensors (DAS) perform distributed and dynamic strain or temperature change measurements by comparing a measured time-domain trace with a previous fiber reference state. Large strain or temperature fluctuations or laser frequency noise impose the need to update such reference, making it necessary to integrate the short-term variation measurements if absolute strain or temperature variations are to be obtained. This has the drawback of introducing a 1/f noise component, as noise is integrated with each cumulative variation measurement, which is detrimental for the determination of very slow processes (i.e., in the mHz frequency range or below). This work analyzes the long-term stability of chirped pulse phase-sensitive optical time domain reflectometry (CP-ΦOTDR) with multi-frequency database demodulation (MFDD) to carry out "calibrated" measurements in a DAS along an unmodified SMF. It is shown that, under the conditions studied in this work, a "calibrated" chirped pulse DAS with a completely suppressed reference update-induced 1/f noise component is achieved, capable of making measurements over periods of more than 2 months with the same set of references, even when switching off the interrogator during the measurement.

Distributed optical fiber sensors (DOFS) allow performing position-resolved measurements of magnitudes that affect an optical fiber, usually, strain or temperature variations [1]–[3]. Among DOFS, distributed acoustic sensors (DAS) deliver dynamic monitoring (at acoustic rates) of such physical magnitudes. While strain is the main parameter to be monitored in DAS, other physical variables such as refractive index, temperature, radiation or electric field can also be measured [4], [5] with the same principle. Time domain DOFS work by sending a pulse of light into the fiber and analyzing the backscattered light as a function of the time of flight [1], [2]. Rayleigh-based DAS systems, in particular, retrieve the backscatter of launched (coherent) optical pulses to measure changes in the optical path experienced by the pulses within the fiber [6]. Since the used pulses are coherent and the system is sensitive to the optical path changes within the pulse length, this technique is known as phase-sensitive optical time-domain reflectometry (ΦOTDR). In ΦOTDR, a local change in the refractive index due to an external perturbation results in a frequency shift in the backscattered light field at the point where the disturbance occurs. Note that in Rayleigh-based sensors, what is measured is a variation in the optical path, which changes both due to temperature and deformation, this causes that strain and temperature effects are indistinguishable in real measurements.

To quantify the applied stimulus on the fiber at acoustic frequencies, it is typically required to measure the phase of the backscattered field [7]–[10]. Quantification of the applied strain or temperature change can also be done using intensity-only measurements by frequency sweeping the laser probe in each measurement [11], [12]. However, dynamic measurements are almost impossible over relatively long fibers by using these techniques. In 2016, the use of chirped pulses in ΦOTDR schemes was proposed [13], allowing single-shot measurements of strain or temperature perturbations using intensity-only measurements [13], [14]. By adding a linear variation of the frequency along the pulse, it is possible to correspond each perturbation-induced frequency shift with a local shift of the trace in the time domain. Thus, the sensors based on chirped-pulse (CP-)ΦOTDR rely on dividing each trace into temporal windows and measuring the temporal displacement of each window with respect to the equivalent window in a reference trace. There are several methods for estimating this time delay, although the most common is cross-correlation [15]. Note that, for the frequency-to-time mapping to remain valid, the perturbation-induced frequency shift is assumed to be much smaller than the chirp-induced bandwidth ($\delta\upsilon$). Practically, this implies a maximum delay in the traces corresponding to 2-4% of the temporal window [13]. Thus, this methodology has the disadvantage that when large disturbances (strain or temperature variations) are measured, the local refractive index profile of the fiber changes so much that the time-delay

estimation approach may no longer be valid [16]. A solution that does not imply the increase of the chirp spectral content (which would increase the detection and acquisition bandwidth requirements) is to update the reference trace and integrate the measurements to obtain absolute values with respect to an initial state of the fiber. However, in this process, the random noise of the measurement is also integrated with each reference update, so a 1/f noise component is introduced. This fact considerably hinders the performing of measurements at low frequencies (<0.1 Hz). And even while modern state-of-the-art processing techniques allow for the 1/f noise to be lowered, the measurement still fundamentally accumulates noise over time and requires continuous uninterrupted acquisitions for long-term measurements [17].

In reference [18], the authors proposed a new method that aims to expand the measurement range (without reference updates) in CP-ΦOTDR sensors. This new method is based on acquiring a database of reference traces at different frequencies of the interrogation laser. Subsequently, for each measured trace, the reference with the maximum similarity is sought to calculate the global frequency shift ($\Delta\upsilon$). Later, the time delay between the measurement and the maximum similarity reference is sought to find the local frequency shift thanks to the chirp-induced time to frequency mapping,

$$\Delta\epsilon/k_\epsilon = \Delta T/k_T = (1/\upsilon_0)(\delta\upsilon/\tau_p \cdot \Delta t + \Delta\upsilon) \qquad (1)$$

being Δt the time delay between the measurement trace and the best correlated reference trace, $\delta\upsilon$ is the chirp spectral content, τ_p the pulse width, υ_o the central frequency of the references array, and k_ϵ and k_T are the strain and temperature constants, respectively. Although very interesting, the work in [18] was only intended to increase the measurable strain rate without updating the reference and, therefore, low time-bandwidth product pulses and few reference frequencies were employed. Moreover, in [18], a random fiber grating array (RFGA) was used as a sensing element, and testing the method in standard, unmodified telecommunication optical fibers remains so far unexplored. In addition, the performance of this architecture at very low frequencies was not studied. Such a study would be fundamental in order to leverage this technique in fields like seismology, where the noise performance at mHz frequencies is critical.

A substantial improvement in the estimation of the global frequency shift ($\Delta\upsilon$) can be achieved by decreasing the frequency spacing with which the multi-frequency database is taken. Being more specific, this spacing must comply with at most 2-3% of the spectral content of the chirp according to the experimental results of [13]. Also note that, by increasing the time-bandwidth product of the pulses, the traces will have more temporal features and therefore the similarity search will be more robust. In this work, we demonstrate that having a sufficiently large database of reference traces acquired with high time-bandwidth product pulses, we can implement the multi-frequency data base demodulation method over a standard telecom fiber. Besides, we show that this method can provide absolute measurements of strain and temperature for long periods of time, even months, without requiring frequency sweeping after the initial calibration.

It is worth noting that the laser frequency slow drifts can be another source of systematic errors at low frequencies. In the literature, one can find techniques to reduce laser noise [19, 20]. Currently, there are commercial lasers with very low frequency drifts, even less than 12.5 MHz (e.g., NKT Koheras Basik X15), which is translated to < 100 nε in terms of strain. In this work, we focus on avoiding 1/f noise due to reference updates in long-term measurements, so we use a laser with low frequency drift. A further improvement of the low-frequency performance in this setup would imply stabilizing the laser frequency using e.g., absolute laser frequency stabilization [21], which is beyond the scope of this work.

In our experiments, we demonstrated long-term and short-term measurements over a standard telecom fiber using a CP-ΦOTDR architecture like the one depicted in Figure 1 with multifrequency database demodulation method (MFDD) [18]. In this scheme, two branches can be distinguished; the upper branch corresponds to the generation of the chirped pulse. A low phase noise laser (linewidth <100 Hz) and long-term wavelength stability of 0.1 pm is used as the light source. This laser emits by default at 1550.12 nm but allows wavelength tuning in steps of 0.1 pm (12.5 MHz). Here, an electro-optical modulator (EOM) and a semiconductor optical amplifier (SOA) are used to generate a chirped pulse with a good extinction ratio from the continuous wave signal of the laser. The EOM is driven by an Arbitrary Waveform Generator (AWG), which generates a 10 ns and 5 GHz chirped pulse with a repetition frequency of 2 kHz. The SOA is used to window the pulses and achieve extremely large (>50dB) extinction ratio. Subsequently, an erbium-doped fiber amplifier (EDFA) and a 0.1 nm band-pass filter are used to amplify the pulse and reduce the noise of the amplified spontaneous emission, respectively. This pulse is sent to the fiber under test (FUT) through an optical circulator. The backscattered trace is fed into to the lower branch of the setup (reception branch). It is first amplified with another EDFA followed by another band pass filter and photo-detected with a 15 GHz bandwidth photodiode. Lastly, the trace is digitized with an oscilloscope at 20 GSa/s. Two variable optical attenuators are used to adjust the pulse and backscatter trace power.

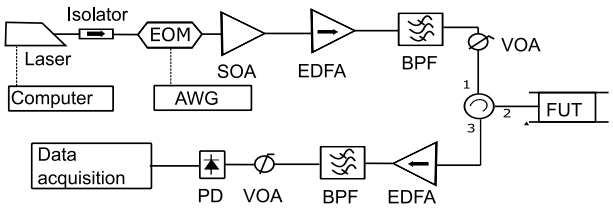

Fig 1. Experimental setup of a DAS system based on CP-ΦOTDR. Electro-optic modulator (EOM), Semiconductor Optical Amplifier (SOA), Erbium-doped Fiber Amplifier (EDFA), Band Pass Filter (BPF), Variable Optical Attenuator (VOA), photo diode (PD).

The most important part of the MFDD method is the calibration process. It consists of the acquisition of a dense reference trace array whose size goes in accordance with the measurement range that is sought. We took a reference array covering 25 GHz, this sweep determines the measurement range of the sensor. Using the known relationship between frequency shift and variation of temperature or strain, we determine that the measurement range for the database taken in this work is 18.7ºC or 165.7 με. The calibration sweep was performed optically, as the laser used allowed for wavelength tuning via software in steps of 0.1pm taking one reference each 30 seconds. For a correct sampling, we enforced a resolution step of < 2% of the chirp spectral content (i.e., 100 MHz in this case) [13], so our frequency step was set to 75 MHz. To also ensure a good SNR in the reference array, each reference trace was

taken by averaging 1000 traces. The system was intended to perform static (i.e. precise in the long-term) and dynamic (i.e. precise in the short term) measurements. Hence, calibration was made along two different fibers: the first one was a 25 km fiber coil and that was immersed in a water bath to stabilize and homogenize the temperature along the fiber; the second one is 4 km of fiber followed by 60 meters wounded around a piezoelectric transducer (PZT), with an optical path displacement of 8.1 μm/V, to be able to induce controlled strain. Note that the calibration of the fibers under test has been done under laboratory conditions, with a known temperature and without applying any deformation to the fiber.

Once the calibration was done, the measurement process consisted of sending pulses to the fiber and acquiring the backscatter traces without averaging. From each detected trace, we estimated the coarse frequency shift by correlating the measurement trace with all the traces in the database. The frequency shift between the central frequency of the database and the frequency of the reference with the highest correlation is known, so by selecting the reference with which it has the highest correlation, we obtain the coarse frequency shift. Subsequently the fine frequency shift by computing the time-delay estimation between the current trace and the maximum correlation trace, according to eq. 1. We used a correlation window with the same size as the pulse width (10 ns), which leads to a spatial resolution of the same size of the pulse width at FWHM [14].

Static measurements were performed by measuring the average temperature of a window of 10 meters of the 25 km of fiber submerged in a water bath over two months, even turning off the interrogator in between. The measurement traces were acquired without averaging, although only sampled at each 30 s, to reduce the dataset size. The obtained results are shown in Figure 2. To verify that the temperature measurement with respect to the fiber calibration instant is correct, a thermocouple has been placed in the center of the fiber roll. A good matching between both measurements has been obtained along the whole period.

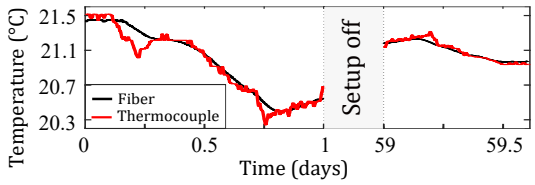

Fig 2. Comparison of temperature measurement with MFDD method and with a thermocouple, absolute measurements are achieved after two months, even turning off the equipment in between. The measurement has been made 2 km from the fiber input end.

The difference between the temperature of the fiber and the thermocouple at the points where the trend changes is due to the different thermal inertia of the two sensors and the different positions of the sensors into the water bucket. This is the first time, to the best our knowledge, that "calibrated" DAS measurements are successfully obtained over such timescales and before and after switching off the interrogator, employing only a single set of reference traces. Note that, while this long-term measurement was performed using a temperature perturbation (due to a logistical impossibility of applying metric strains under millikelvin temperature-controlled conditions in our lab), there is extensive literature documenting that the perturbations applied by a strain or temperature are fundamentally similar in phase-sensitive OTDR and therefore this long-term measurement should also be seen validatory of the possibility of measuring of long-term strain.

For the dynamic measurements, 60 meters of fiber were wrapped around a calibrated PZT cylinder placed at the end of a 4 km fiber coil. We applied a sine-varying voltage of 0.05 Hz and 22 Vpp to the PZT (which is equivalent to a ~3 με peak-to-peak strain modulation in the fiber), and we took unaveraged trace measurements with a repetition rate of 0.5 Hz. In Figure 3, we can see the measurements along the 60 meters of perturbed fiber, where we can very well distinguish the three layers of fiber coil around the PZT cylinder. This implies not only a good determination of the strain modulation (as in conventional DAS systems) but also a good determination of the background (DC) contribution to the perturbation introduced by the existence of a temperature gradient of ≈0.1° C between each of the 3 layers of 20 meters of fiber wrapped around the PZT (equivalent to a strain perturbation of ≈1 με in ΦOTDR systems [11]). Note that the perturbation offset determination of each layer would have been impossible with the conventional DAS methodology due to the 1/f noise of each spatial measurement window.

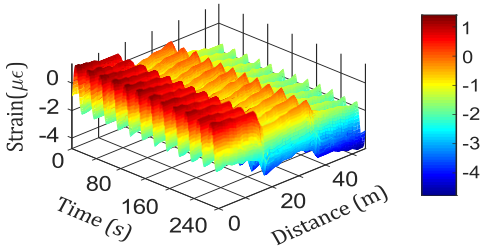

Fig 3. Strain measurements along the fiber Vs time.

The here described technique allows CP-ΦOTDR measurements to be made without updating the reference traces for long periods. In traditional CP-ΦOTDR systems, the need for updating references leads to an error accumulation over time (translated into a 1/f noise in the spectral domain). Hence, measuring low-frequency strain or temperature variations becomes extremely challenging. The multi-frequency reference database allows absolute measurements in CP-ΦOTDR without error accumulation, cancelling the reference update-induced 1/f noise. To verify this, a vibration of 0.05 Hz has been measured over 6 hours. Furthermore, to demonstrate the operation of the MFDD method at very low frequencies, a sinusoidal modulation at the laser frequency of 0.008 Hz has been introduced, which is known to be indiscernible from a strain or temperature modulation in ΦOTDR based sensors [11]. In figure 4.a the median of the measurement along the PZT fiber positions is compared using conventional chirped pulse DAS with single-reference updates, and using the fixed reference set (MFDD), with MFDD method the random walk (1/f noise) is eliminated. In figure 4.b we see the standard deviation (STD) of the measurements along the PZT fiber. The STD with the MFDD method remains low, while with the traditional CP-DAS, the STD increases with the square root of the reference updates. In fig. 4.c the Amplitude Spectral Density (ASD) of the measurement is compared both methods and, as it is visible, the low-frequency noise induced by the process of updating references has virtually disappeared in the MFDD case. The bump at sub-mHz frequencies is related to real temperature fluctuations

in the fiber over the 6 hours of measurement, measured by the thermocouple. We can see how with the MFDD method we can clearly distinguish the 0.008 Hz modulation, while with the traditional method, this modulation is masked by 1/f noise.

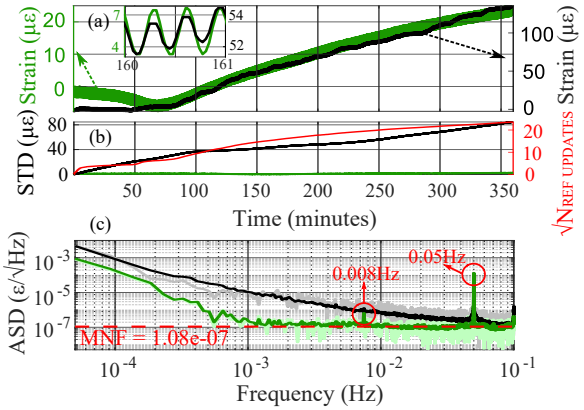

Fig 4. (a) Median characteristic measurement using MFDD method (green) and using conventional CP-DAS (black). Inset, one minute zoom of the sinusoidal strain perturbation. (b) STD of PZT fiber positions using MFDD (green) and using traditional CP-DAS (black). In red, the square root of the number of times the reference is updated using traditional CP-DAS. (c) Median ASD of a conventional CP-DAS (strong black line) and MFDD (strong green line). Light colored lines are the ASD of an example fiber point (z = 4011 m). Note that both methods differ only in the processing, as it is the same physical measurement, using the same optical traces.

Note that to achieve measurements along 6 hours, the acquisition frequency was significantly lowered in order to reduce the dataset size. This implies a general loss of sensitivity with respect to the normal working conditions of a CP-DAS (sampled at kHz), which easily reaches sensitivities well below the nε/√Hz. Additionally, note that the spatial resolution here used (1 meter) is one order of magnitude lower than that of previous studies, aimed at maximizing the strain sensitivity [22]. To make a fair comparison, the measurements in Figure 4 have been acquired under the same acquisition conditions. According to [22], the Cramer Rao Lower Bound (CRLB) for a DAS system with reference updates in such conditions sets sensitivities of $\sim 2.5 \cdot 10^{-8}\ \epsilon/\sqrt{\text{Hz}}$ (i.e. $\tau_p = 10ns$, $B_s = 5GHz$, $\upsilon_0 = 193.4THz$, $f_{acq} = 0.5Hz$, 3 dB SNR), which agrees with the obtained sensitivity values (note that the median noise floor (MFN) for the MFDD method is kept near $10^{-7}\ \epsilon/\sqrt{\text{Hz}}$ for frequencies above 10^{-3}Hz; and below said frequency the system noise is dominated by physical temperature drifts of the fiber wrapped around the PZT). Indeed, it is shown how the 1/f noise introduced by the reference updating process disappears using the initial reference set, instead of using the traditional integration of shot-to-shot variation measurements, which require constant reference updates of a single fiber reference state.

To sum up, this letter describes a measurement technique based on CP-ΦOTDR that makes use of a database of references taken at the beginning of the measurement process, instead of the usual reference update procedure. This allows the DAS equipment and fiber to be calibrated under initial strain and temperature conditions. The elimination of the reference update procedure in CP-DAS yields basically to a complete cancellation of the 1/f noise component associated to noise integration in each reference update. The same set of references has been used to acquire temperature along two months with valid ("calibrated") results, even switching off the interrogator during the measurement. This implies a major change in DAS as long term, virtually absolute measurements could be done with respect to an initial (known) condition. Static and dynamic measurements have been performed, in both cases obtaining good results in agreement with the applied stimuli. The complete cancellation of reference update noise in the CP-ΦOTDR technique together with active stabilization of the laser frequency could enable a new family of interrogators not available so far, pointing to potential advances in the field of seismology, where extremely low frequencies would be measured with relatively good accuracies over long distances.

Funding. Comunidad de Madrid and FEDER Program under grant SINFOTON2-CM:S2018/NMT-4326, MCIN/AEI/10.13039/501100011033 and by the European Union NextGenerationEU/PRTR program, under project PSI ref. PLEC2021-007875, the Spanish Government under projects RTI2018–097957-B-C31, and RTI2018–097957-B-C33. M.R.F.R. acknowledge financial support from the Spanish MICINN under contract no. IJC2018–035684-I. P.J.V.M. acknowledge the UAH-FPI program. 2020/00198/001 - UAH INFR. A 2020-007.

Data availability. Data underlying the results presented in this paper are not publicly available at this time but may be obtained from the authors upon reasonable request.

Disclosures. The authors declare no conflicts of interest.

REFERENCES

1. A. H. Hartog, Florida (USA): CRC Press: Boca Raton, 2017.
2. P. Lu et al., Appl. Phys. Rev., vol. 6, no. 4, p. 041302, 2019.
3. X. Bao, D. P. Zhou, C. Baker, and L. Chen, J. Light. Technol., vol. 35, no. 16, pp. 3256–3267, 2017.
4. R. Magalhães et al., Opt. Express, vol. 27, no. 4, pp. 4317–4328, 2019.
5. R. Magalhães et al., Sensors (Switzerland), vol. 20, no. 16, pp. 1–13, 2020.
6. L. B. Liokumovich, N. A. Ushakov, O. I. Kotov, M. A. Bisyarin, and A. H. Hartog, J. Light. Technol., vol. 33, no. 17, pp. 3660–3671, 2015.
7. M. S. Erkilinç et al., J. Light. Technol., vol. 34, no. 8, pp. 2034–2041, 2016.
8. H. Gabai and A. Eyal, Opt. Lett., vol. 41, no. 24, pp. 5648–5651, 2016.
9. L. M. Parker et al., Seismol. Res. Lett., vol. 89, no. 5, pp. 1629–1640, 2018.
10. S. Liehr, Y. S. Muanenda, S. Münzenberger, and K. Krebber, Opt. Express, vol. 25, no. 2, pp. 720–729, 2017.
11. Y. Koyamada, M. Imahama, K. Kubota, and K. Hogari, J. Light. Technol., vol. 27, no. 9, pp. 1142–1146, 2009.
12. S. Liehr, S. Münzenberger, K. Krebber, Opt. Express 26, 10573-10588, 2018.
13. J. Pastor-Graells, H. F. Martins, A. Garcia-Ruiz, S. Martin-Lopez, and M. Gonzalez-Herraez, Opt. Express, vol. 24, no. 12, pp. 13121–13133, 2016.
14. M. R. Fernández-Ruiz, H. F. Martins, L. Costa, et al, J. Light. Technol., vol. 36, no. 23, pp. 5690–5696, 2018.
15. H. D. Bhatta et al., J. Light. Technol., pp. 1–8, 2019.
16. L. Zhang, L. Costa, Z. Yang, M. A. Soto, M. Gonzalez-Herraez, and L. Thévenaz, J. Light. Technol., vol. 37, no. 18, pp. 4710–4719, 2019.
17. R. Magalhães, T. Neves, L. Scherino, et al, J. Lightwave Technol, vol. 40, no. 12, pp. 3916-3922, 15 June15, 2022.
18. Y. Wang, P. Lu, S. Mihailov, L. Chen, and X. Bao, Opt. Lett., vol. 45, no. 21, pp. 6110–6113, 2020.
19. M. R. Fernández-Ruiz, J. Pastor-Graells, H. F. Martins, et al, J. Lightwave Technol. 36, 979-985 (2018)
20. Y. Wang, P. Lu, S. Mihailov, L. Chen, and X. Bao, Opt. Lett. 46, 789-792 (2021)
21. X. Lu, M. A. Soto, and L. Thévenaz, Proc. SPIE 9157, 23rd International Conference on Optical Fibre Sensors, 91573R (2 June 2014)
22. L. Costa, H. F. Martins, S. Martín-López, M. R. Fernández-Ruiz, and M. González-Herráez, J. Lightwave Technol. 37, 4487-4495 (2019)

REFERENCES

1. A. H. Hartog, An introduction to distributed fiber sensors. Florida (USA): CRC Press: Boca Raton, 2017.
2. P. Lu et al., “Distributed optical fiber sensing: Review and perspective,” Appl. Phys. Rev., vol. 6, no. 4, p. 041302, 2019.
3. X. Bao, D. P. Zhou, C. Baker, and L. Chen, “Recent Development in the Distributed Fiber Optic Acoustic and Ultrasonic Detection,” J. Light. Technol., vol. 35, no. 16, pp. 3256–3267, 2017.
4. R. Magalhães et al., “Fiber-based distributed bolometry,” Opt. Express, vol. 27, no. 4, pp. 4317–4328, 2019.
5. R. Magalhães et al., “Towards distributed measurements of electric fields using optical fibers: Proposal and proof-of-concept experiment,” Sensors (Switzerland), vol. 20, no. 16, pp. 1–13, 2020.
6. L. B. Liokumovich, N. A. Ushakov, O. I. Kotov, M. A. Bisyarin, and A. H. Hartog, “Fundamentals of Optical Fiber Sensing Schemes Based on Coherent Optical Time Domain Reflectometry: Signal Model under Static Fiber Conditions,” J. Light. Technol., vol. 33, no. 17, pp. 3660–3671, 2015.
7. M. S. Erkilinç et al., “Polarization-insensitive single-balanced photodiode coherent receiver for long-reach WDM-PONs,” J. Light. Technol., vol. 34, no. 8, pp. 2034–2041, 2016.
8. H. Gabai and A. Eyal, “On the sensitivity of distributed acoustic sensing,” Opt. Lett., vol. 41, no. 24, pp. 5648–5651, 2016.
9. L. M. Parker et al., “Active-source seismic tomography at the brady geothermal field, Nevada, with dense nodal and fiber-optic seismic arrays,” Seismol. Res. Lett., vol. 89, no. 5, pp. 1629–1640, 2018.
10. S. Liehr, Y. S. Muanenda, S. Münzenberger, and K. Krebber, “Relative change measurement of physical quantities using dual-wavelength coherent OTDR,” Opt. Express, vol. 25, no. 2, pp. 720–729, 2017.
11. Y. Koyamada, M. Imahama, K. Kubota, and K. Hogari, “Fiber-optic distributed strain and temperature sensing with very high measurand resolution over long range using coherent OTDR,” J. Light. Technol., vol. 27, no. 9, pp. 1142–1146, 2009.
12. Sascha Liehr, Sven Münzenberger, and Katerina Krebber, "Wavelength-scanning coherent OTDR for dynamic high strain resolution sensing," Opt. Express 26, 10573-10588 (2018)
13. J. Pastor-Graells, H. F. Martins, A. Garcia-Ruiz, S. Martin-Lopez, and M. Gonzalez-Herraez, “Single-shot distributed temperature and strain tracking using direct detection phase-sensitive OTDR with chirped pulses,” Opt. Express, vol. 24, no. 12, pp. 13121–13133, 2016.
14. M. R. Fernández-Ruiz, H. F. Martins, L. Costa, S. Martin-Lopez, and M. Gonzalez-Herraez, “Steady-Sensitivity Distributed Acoustic Sensors,” J. Light. Technol., vol. 36, no. 23, pp. 5690–5696, 2018.
15. H. D. Bhatta et al., “Dynamic Measurements of 1000 microstrains using Chirped-pulse Phase Sensitive Optical Time Domain Reflectometry (CP-ΦOTDR),” J. Light. Technol., pp. 1–8, 2019.
16. L. Zhang, L. Costa, Z. Yang, M. A. Soto, M. Gonzalez-Herraez, and L. Thévenaz, “Analysis and Reduction of Large Errors in Rayleigh-based Distributed Sensor,” J. Light. Technol., vol. 37, no. 18, pp. 4710–4719, 2019.
17. R. Magalhães, T. Neves, L. Scherino, S. Martin-Lopez and H. F. Martins, "Reaching Long-Term Stability in CP-φOTDR," in Journal of Lightwave Technology, vol. 40, no. 12, pp. 3916-3922, 15 June15, 2022, doi: 10.1109/JLT.2022.3150274.
18. Y. Wang, P. Lu, S. Mihailov, L. Chen, and X. Bao, “Strain measurement range enhanced chirped pulse ϕ-OTDR for distributed static and dynamic strain measurement based on random fiber grating array,” Opt. Lett., vol. 45, no. 21, pp. 6110–6113, 2020.
19. M. R. Fernández-Ruiz, J. Pastor-Graells, H. F. Martins, A. Garcia-Ruiz, S. Martin-Lopez, and M. Gonzalez-Herraez, "Laser Phase-Noise Cancellation in Chirped-Pulse Distributed Acoustic Sensors," J. Lightwave Technol. 36, 979-985 (2018)
20. Y. Wang, P. Lu, S. Mihailov, L. Chen, and X. Bao, "Ultra-low frequency dynamic strain detection with laser frequency drifting compensation based on a random fiber grating array," Opt. Lett. 46, 789-792 (2021).
21. Xin Lu, Marcelo A. Soto, and Luc Thévenaz "MilliKelvin resolution in cryogenic temperature distributed fibre sensing based on coherent Rayleigh scattering", Proc. SPIE 9157, 23rd International Conference on Optical Fibre Sensors, 91573R (2 June 2014)
22. Luís Costa, Hugo F. Martins, Sonia Martín-López, María R. Fernández-Ruiz, and Miguel González-Herráez, "Fully Distributed Optical Fiber Strain Sensor With 10−12 ε/ √ Hz Sensitivity," J. Lightwave Technol. 37, 4487-4495 (2019)